Tensile Behavior of Weathered Thermally Bonded Polypropylene Geotextiles: Analysis Using Constitutive Models

José Ricardo Carneiro, Ph.D.[1]; António Miguel Paula, Ph.D.[2]; and Margarida Pinho-Lopes, Ph.D.[3]

Abstract: Weathering agents can significantly affect the mechanical response of geotextiles, particularly when long exposure periods are involved. Usually, in design, changes in the mechanical behavior of geotextiles are represented by reduction factors for their tensile strength. However, their full tensile force versus elongation response can be affected. The main aim of this work was to contribute to defining simple procedures to estimate tensile force versus elongation curves for weathered samples of geotextiles. The tensile response of two thermally bonded polypropylene geotextiles, before and after natural and artificial weathering, was assessed experimentally and analyzed using different constitutive models: polynomial (Orders 4 and 6) and hyperbolic. The influence of weathering on the mechanical response of the geotextiles was analyzed, polynomial and hyperbolic models for representing the tensile force versus elongation response were adopted and their parameters derived, and simple relations were implemented to estimate model parameters for weathered samples. Results revealed the occurrence of changes in the tensile behavior of the geotextiles, both under natural and artificial weathering conditions. Both groups of models fitted the experimental data properly. The Order 4 and 6 polynomial models are shown to have limited application, as the model parameters had no link to the tensile properties of the geotextiles. By contrast, the parameters of the hyperbolic model were linked to the tensile properties, particularly if affected by correction factors. The hyperbolic model parameters of the weathered samples were estimated using the model parameters of the reference samples and the reduction factors to allow for weathering (initial stiffness and tensile strength). These estimates proved to be adequate for representing the tensile response of weathered samples, particularly for low ranges of elongation. Finally, a simple procedure to represent the tensile response of weathered geotextiles was proposed. This procedure has shown promise in generating realistic tensile versus elongation curves. **DOI: 10.1061/JMCEE7.MTENG-15740.**

Author keywords: Geotextile; Weathering; Ultraviolet (UV) radiation; Durability; Constitutive models; Tensile response.

Introduction

Geotextiles are well-established materials in civil engineering. These materials, mostly made from synthetic polymers, are versatile, being suitable for performing a wide range of functions. The possible applications of geotextiles are varied (Koerner 2012), including road infrastructure (Giroud et al. 2022), drainage systems (Han 2015), erosion control works (Sprague and Sprague 2016), or landfills (Touze-Foltz et al. 2016; Rowe 2020). In most applications, they are expected to perform functions for a long time, which means they need high levels of durability.

Geotextiles can suffer degradation in the installation phase and during service life. In the installation phase, damage can result from installation procedures as well as exposure to atmospheric agents (when materials are not readily covered by soils or liquids). During service life, many agents can influence the behavior of geotextiles with examples including chemicals, high temperatures, atmospheric agents (e.g., solar radiation), abrasion, or creep (Greenwood et al. 2016; Shukla 2016). As with other polymeric materials, geotextiles are prone to oxidation, which usually has a negative impact on their properties. The oxidation process can be promoted by temperature (thermo-oxidation) or by ultraviolet (UV) radiation (photo-oxidation) (Maier and Calafut 1998; Feldman 2002). Thus, if it cannot be avoided, the exposure of geotextiles to solar radiation should be kept to a minimum.

The resistance of geotextiles to solar radiation and other weathering agents is normally evaluated in the laboratory, under controlled and accelerated degradation conditions (Carneiro et al. 2011; Koerner et al. 2017; Filho et al. 2019). To this end, international standardization institutions, such as the American Society for Testing and Materials or the European Committee for Standardization, have developed EN 12224 (CEN 2000) and ASTM D4355 (ASTM 2021). These methods provide relatively fast results, but they have limitations, one of which is the difficulty in extrapolating the results obtained in the laboratory to field conditions. As an alternative,

[1]Postdoctroal Researcher, CONSTRUCT, Dept. of Civil Engineering, Faculty of Engineering, Univ. of Porto, Rua Dr. Roberto Frias, Porto 4200-465, Portugal (corresponding author). ORCID: https://orcid.org/0000-0003-0552-4076. Email: rcarneir@fe.up.pt

[2]Assistant Professor, Instituto Politécnico de Bragança, Campus de Santa Apolónia, Bragança 5300-253, Portugal; Researcher, CONSTRUCT, Dept. of Civil Engineering, Faculty of Engineering, Univ. of Porto, Rua Dr. Roberto Frias, Porto 4200-465, Portugal; Researcher, RISCO, Dept. of Civil Engineering, Univ. of Aveiro, Campus Universitário de Santiago, Aveiro 3810-193, Portugal. ORCID: https://orcid.org/0000-0003-4788-8644. Email: mpaula@ipb.pt

[3]Assistant Professor, RISCO, Dept. of Civil Engineering, Campus Universitário de Santiago, Aveiro 3810-193, Portugal; Visiting Academic in Geomechnaics, Faculty of Engineering and Physical Sciences, Univ. of Southampton, Boldrewood Innovation Campus, Southampton SO16 7QF, UK. ORCID: https://orcid.org/0000-0003-0808-6307. Email: mlopes@ua.pt

Note. This manuscript was submitted on October 4, 2022; approved on May 3, 2023; published online on September 25, 2023. Discussion period open until February 25, 2024; separate discussions must be submitted for individual papers. This paper is part of the ***Journal of Materials in Civil Engineering***, © ASCE, ISSN 0899-1561.

field tests can be conducted, where the geotextiles are exposed to weathering under natural degradation conditions (Hsieh et al. 2006; Carneiro and Lopes 2017; Aparicio-Ardila et al. 2021). However, these tests are often time-consuming, typically taking a few months or years, which limits their use as screening tests.

The degradation of geotextiles in weathering tests is normally assessed by monitoring changes in their tensile behavior. Based on changes in tensile strength, a reduction factor (accounting for the effects of weathering) can be defined to use in the design (ISO 2007; BSI 2010). ISO/TR 20432 (ISO 2007), a guide for determining the long-term strength of geosynthetics for soil reinforcement, mentions that it is not necessary to apply a reduction factor if exposure to UV radiation is less than 12 h. However, if exposure time is longer, then the geosynthetics should be submitted to an accelerated weathering test such as EN 12224 (CEN 2000), and the reduction factor to be applied will be based on the test results. Typical reduction factors allowing for weathering are often conservative but may provide a good initial estimate.

In addition to tensile behavior, other mechanical properties of geotextiles (e.g., puncture behavior) (Carneiro and Lopes 2017), as well as physical properties (Carneiro et al. 2019; Aparicio-Ardila et al. 2021), were also monitored in weathering tests. Other techniques used to detect UV degradation in geotextiles include spectrophotometry (Filho et al. 2019), thermal analysis (Aparicio-Ardila et al. 2021; Franco et al. 2022), liquid chromatography (Valente et al. 2011), and scanning electron microscopy (Carneiro et al. 2019; Aparicio-Ardila et al. 2021).

The tensile strength is often a key design property of geotextiles. The values adopted in design correspond to those of the as-received material affected by relevant reduction factors (e.g., allowing for the effects of weathering). However, the overall tensile behavior of geotextiles can be affected by degradation agents. Thus, the design should include the complete tensile force versus elongation response of the degraded materials. To contribute to a more realistic design, it is key to represent geotextiles and their response using models that capture the tensile load versus elongation curves after degradation. In the design and analysis of geotextiles and of structures where they are included, numerical methods, such as the finite element method, have become widespread. However, in most cases, geotextiles are represented by oversimplistic constitutive relations, such as linear elastic models, and without any allowance for degradation. For both ultimate and service conditions, more realistic constitutive relations can be used. Thus, adopting nonlinear elastic–plastic models and considering the influence of degradation agents on the tensile response of geotextiles can contribute to more realistic and economic designs.

There are constitutive models that can capture the tensile behaviour of geosynthetics (Perkins 2000; Bathurst and Kaliakin 2005). Such models tend to be phenomenological, and the model parameters are obtained by curve fitting of experimental data. One of the aims of this paper is to contribute to defining simple procedures that enable deriving model parameters allowing for degradation, while using experimental data available for the design of geotextiles. These are novel and essential contributions to this topic.

The literature offers only a few research studies using this approach. Paula and Pinho-Lopes (2021) and Lombardi et al. (2022) used a similar approach to analyze the short-term behavior of other geosynthetics (geotextiles, geogrids, and geocomposites) and the influence of different durability agents (namely, mechanical) on their tensile response, constitutive models, and model parameters. The authors have estimated model parameters for several geosynthetics, as-received and damaged, and related the model parameters for the damaged samples to those of the as-received samples combined with their tensile properties and relevant reduction factors. These works focused on the effect of mechanical and abrasion damage of geosynthetics, acting separately and sequentially. The properties and reduction factors applied for representing the tensile response of geosynthetics included the tensile strength and the stiffness (initial and for predefined elongation values, e.g., 2% and 5%).

However, no studies were found in which constitutive models were used to represent the full tensile force versus elongation response of weathered geotextiles. This paper aims to contribute to defining simple tensile force versus elongation curves for weathered samples of geotextiles. These models can then be implemented in software using finite element or finite differences methods. Ultimately, this approach will enable representing the tensile response of geotextiles more realistically, which is particularly relevant for elongations typical of service.

The specific objectives of this paper are to

1. Assess the influence of weathering on the tensile force versus elongation response of two geotextiles, thus analyzing the influence of type of weathering (natural and artificial) and characteristics of the geotextiles;
2. Evaluate if simple constitutive models can represent the tensile force versus elongation response, deriving the model parameters for reference and weathered samples; and
3. Implement simple relations that enable estimating model parameters for weathered samples, using values of the tensile properties of reference and weathered samples.

Materials and Methods

Geotextiles

This work was conducted with two nonwoven thermally bonded geotextiles made from continuous polypropylene (PP) filaments with a diameter of 40 to 50 μm (Fig. 1). The geotextiles (designated in this work by GT165 and GT375) were gray in color, from the same product range (they had different tensile behavior and different physical properties), and UV stabilized (stabilization package not disclosed by the manufacturer). GT165 and GT375 were chosen to represent examples of thermally bonded geotextiles used in geotechnical applications. The masses per unit area (μ_A, in g/m^2) and thicknesses under 2 kPa (t, in mm) of the geotextiles can be found in Table 1. The previous properties were determined according to EN ISO 9864 (CEN 2005b) and EN ISO 9863-1 (CEN 2016), respectively. Tensile properties of the geotextiles are presented in "Tensile Results."

The sampling and preparation of test-specimens followed the guidelines of EN ISO 9862 (CEN 2005a). For each geotextile, the specimens were treated under four different conditions: (1) undamaged (reference sample); (2) exposed to six months of natural weathering (NW-6 sample); (3) exposed to 12 months of natural weathering (NW-12 sample); and (4) exposed to artificial weathering (AW sample).

Tensile Tests

The geotextiles (reference and weathered samples) were characterized by tensile tests according to EN 29073-3 (CEN 1992). These tests were performed in a tensile machine from Lloyd Instruments (model LR50K). For each sample, five specimens were tested at a speed of 100 mm/min. The specimens had a width of 50 mm and length of 400 mm (length between jaws of 200 mm). Elongation was measured based on the relative displacement of the jaws.

The parameters determined in the tensile tests (values in the machine direction of production) were tensile strength (T_{max}, in kN/m) and corresponding elongation (ε_{Tmax}, in %), secant stiffness at 2% elongation ($J_{s2\%}$, in kN/m), and secant stiffness at 5%

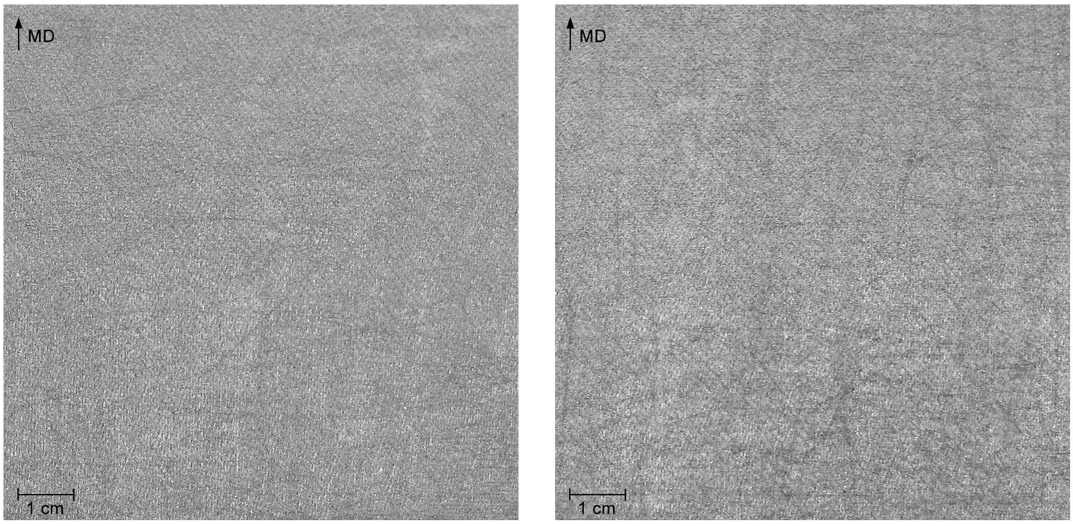

Fig. 1. Thermally bonded geotextiles: (a) GT165; and (b) GT375. (Arrow indicates the manufacturing direction, MD.)

Table 1. Main characteristics of GT165 and GT375

Geotextile	GT165	GT375
Polymer	Polypropylene (UV stabilized)	
μ_A (g/m^2)	164 ± 8	380 ± 10
t (mm)	0.46 ± 0.02	0.83 ± 0.02

Note: Average values and 95% confidence intervals.

elongation ($J_{s5\%}$, in kN/m). The results (average values of five specimens) are presented with 95% confidence intervals.

Weathering Tests

Natural Weathering

The exposure site was located in Maia, Portugal, at latitude 41°13'N and longitude 8°39' W (49 m above sea level). The materials were exposed facing south with an inclination of 30°. Two exposure periods were considered: 6 and 12 months. The specimens had a width of 50 mm and length of 400 mm (exposed area of 50 × 200 mm).

The main climate parameters were continuously monitored during the field exposure (Table 2). The solar radiant energy was measured between 300 and 3,000 nm, with no information available separately for the UV region. Taking into account the intervals provided in EN 13362 (CEN 2013) and Greenwood et al. (2016) (respectively, 6% to 9% and 5% to 10%), the UV radiant energy was estimated to be 7.5% of the solar radiant energy.

Table 2. Climate parameters of the field exposure site

Exposure period (months)	$T_{air,avg}$ (°C)	$T_{air,min}$ (°C)	$T_{air,max}$ (°C)	E[a] (MJ/m^2)	E_{UV}[b] (MJ/m^2)	P (mm)
0–6	13.6	4.8	23.4	1,344	101	815
7–12	22.0	13.8	31.1	3,999	300	279
0–12	17.8	4.8	31.1	5,343	401	1,094

Note: $T_{air,avg}$ = daily average air temperature: average; $T_{air,min}$ = daily average air temperature: minimum; $T_{air,max}$ = daily average air temperature: maximum; E = accumulated solar radiant energy; E_{UV} = accumulated UV radiant energy; and P = accumulated precipitation.
[a]Measured between 300 and 3,000 nm.
[b]Estimated as being 7.5% of the accumulated solar radiant energy.

Artificial Weathering

The artificial weathering tests (exposure to alternated cycles of UV radiation and water spray) were conducted on a laboratory weatherometer, i.e., the QUV Weathering Tester (Q-Panel Lab Products, model QUV/spray). The geotextiles (specimens with a width of 50 mm and a length of 400 mm; exposed area of 50 × 200 mm) were exposed to the following weathering cycle:

1. UV radiation (duration: 5 h; temperature: 50°C).
2. Water spray (duration: 10 min; water at room temperature).
   (Return to Step 1.)

The geotextiles were exposed in the laboratory weatherometer for 362 h (≈15 days), which corresponded to about 70 weathering cycles (each cycled lasted for 5 h and 10 min). The UV radiation was provided by fluorescent UVA-340 lamps operating with an irradiance of 0.68 W/m^2 at 340 nm. These lamps were turned off during the spray step. The accumulated UV radiant exposure (between 290 and 400 nm) was 50 MJ/m^2. The water flow in the spray step was 5 L/min. The test conditions closely followed EN 12224 (CEN 2000). The main deviation, which is expected to have little impact on the results, was the reduction of the spray step duration from 60 to 10 min. This was necessary due to limitations in the laboratory, namely, in the water purification system (the weatherometer requires the use of purified water to prevent clogging of sprinklers).

Constitutive Models

Mathematical frameworks used to describe the mechanical behavior of materials are designated as constitutive models. Such models depend on a variety of parameters, often representing mechanical characteristics of the material. These parameters, constant values, must be quantified adequately, to be adopted in the equations of the relevant constitutive models. Thus, the calibration of the constitutive model implies the mechanical characterization of the material (Buljak and Ranzi 2021).

The tensile behavior of GT165 and GT375 was analyzed using constitutive equations, representing the tensile force (T) versus elongation (ε) response. The constitutive equations considered

Table 3. Tensile properties of GT165 and GT375 before and after the weathering tests

Geotextile	Sample	T_{max} (kN/m)	ε_{Tmax} (%)	$J_{s2\%}$ (kN/m)	$J_{s5\%}$ (kN/m)
GT165	Reference	9.65 ± 0.71	34.7 ± 9.4	180.88 ± 10.87	113.15 ± 4.71
	NW-6	9.04 ± 0.35	25.1 ± 4.6	175.65 ± 14.48	110.68 ± 7.83
	NW-12	6.39 ± 0.26	11.7 ± 0.7	159.79 ± 8.49	97.27 ± 3.94
	AW	7.50 ± 1.84	10.7 ± 4.6	186.09 ± 18.32	117.10 ± 11.22
GT375	Reference	26.95 ± 1.68	40.9 ± 3.4	426.23 ± 31.70	268.07 ± 17.87
	NW-6	26.63 ± 2.42	37.1 ± 3.8	428.96 ± 35.73	266.83 ± 23.02
	NW-12	20.70 ± 0.35	22.7 ± 0.9	407.55 ± 8.85	243.95 ± 4.66
	AW	25.86 ± 1.39	31.7 ± 3.7	421.03 ± 19.86	267.88 ± 13.64

Note: Average values and 95% confidence intervals.

herein represent the time-independent tensile response and correspond to simple models: polynomial and hyperbolic. These models are considered appropriate simplifications of the short-term tensile response of geosynthetics (Bathurst and Kaliakin 2005).

The polynomial model is based on a polynomial constitutive equation [Eq. (1)] of order n, where the model parameters are the coefficients a_i. Herein, two different polynomial equations were used: Order 4 and Order 6. These were chosen so that: (1) they meet the conditions of the Weierstrass approximation theorem (Pinkus 2000), which states that every continuous function defined on a given interval can be estimated, as closely as needed, by a polynomial equation; (2) high-order polynomial equations are used, enabling higher efficiency of estimation relative to lower-order polynomials; (3) the order of the polynomial is even; and (4) the polynomial includes inflection points

$$T = \sum_{i=0}^{n} a_i \varepsilon^i \tag{1}$$

Two different hyperbolic-based models can be used to represent the tensile response of geosynthetics, depending on the type of experimental behavior observed (Liu and Ling 2006): Type A, decreasing tangent stiffness with increasing elongation; Type B, initial decrease of tangent stiffness, for low elongations, followed by an increase of that stiffness, with increasing elongation. GT165 and GT375 exhibited a Type A response; thus, hyperbolic models [Eq. (2)] were also used in this work. The physical meaning of model parameters is represented in Eqs. (3) and (4): a depends on the initial tangent stiffness (J_i); b is the asymptote of the hyperbola and is related to the tensile strength of the geotextile, T_{max}

$$T = \frac{\varepsilon}{a + b\varepsilon} \tag{2}$$

$$J_i = \frac{1}{a} \qquad \varepsilon \to 0 \tag{3}$$

$$T_{max} = \frac{1}{b} \qquad \varepsilon \to \varepsilon_{T_{max}} \tag{4}$$

The instantaneous tangent stiffness, J, can be obtained by differentiating the constitutive equation [Eqs. (1) or (2), for polynomial and hyperbolic models] with respect to elongation [Eqs. (5) and (6), respectively, for polynomial and hyperbolic models]

$$J = \sum_{i=1}^{n} a_i \varepsilon^{i-1} \tag{5}$$

$$J = \frac{a}{(a + b\varepsilon)^2} \tag{6}$$

Tensile Results

The weathering tests (under natural and artificial conditions) caused some changes in the tensile behavior of the geotextiles. The tensile properties of the reference and weathered samples of GT165 and GT375 can be found in Table 3. In order to complement the information presented in Table 3, Fig. 2 illustrates the representative tensile force versus elongation curves of the geotextiles before and after the weathering tests. These curves correspond to the curves of the individual specimens that had the tensile behavior closest to the average of the five specimens tested (designated as representative).

Regarding GT165, the T_{max} of the NW-6 sample was slightly lower (6.3%) than that of the reference sample. The increase of the exposure time to 12 months resulted in a more pronounced change in T_{max}, with the NW-12 sample having a T_{max} 33.8% lower than the reference sample. This reduction was not anticipated, as no visible (to the naked eye) damage was found on GT165 after 12 months.

The natural weathering tests also had an impact on the ε_{Tmax} of GT165. For both samples, ε_{Tmax} decreased after these tests, the decrease being more remarkable in the NW-12 sample. Regarding $J_{s2\%}$ and $J_{s5\%}$, no relevant changes were found in these parameters in the NW-6 sample. By contrast, slight reductions were observed in the NW-12 sample (11.7% and 14.0%, respectively, for $J_{s2\%}$ and $J_{s5\%}$). Generally speaking, six months of natural weathering did not have a pronounced impact on the tensile behavior of GT165.

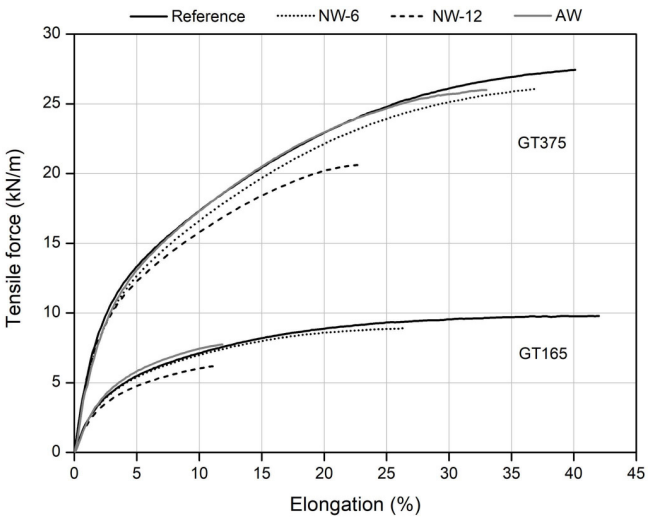

Fig. 2. Representative tensile force versus elongation curves of GT165 and GT375 before and after the weathering tests.

Indeed, considering the 95% confidence intervals, its tensile properties did not change significantly. In the case of 12 months, the conclusions are different, with meaningful changes observed in the tensile behavior of GT165.

As with GT165, GT375 did not show relevant changes in its tensile properties after six months of natural weathering. The small reductions found in T_{max}, ε_{Tmax}, and $J_{s5\%}$ are meaningless when considering the 95% confidence intervals. The increase of the exposure time to 12 months led to a decrease in T_{max} (23.2%) and ε_{Tmax} (from 40.9% to 22.7%). The $J_{s2\%}$ and $J_{s5\%}$ of the NW-12 sample were slightly lower (4.4% and 9.0%, respectively) than those of the reference sample but not significantly different when considering the 95% confidence intervals.

The weathering resistance of GT375 was not much different from that of GT165 but was slightly higher. Both materials showed relatively good resistance to six months of natural weathering, with no relevant differences between them. However, the increase of the exposure time had a slightly greater impact on GT165 than on GT375. Indeed, reductions in T_{max} of 33.8% and 23.2% were found, respectively, for these geotextiles after 12 months. The difference may be explained by the higher mass per unit area and thickness of GT375. Another possibility is the stabilization package differs in the two geotextiles. As will be noted, in the artificial weathering tests, GT375 was also slightly less affected than GT165.

The period from seven to 12 months was more damaging to GT165 and GT375 than the period zero to six months. As can be seen in Table 2, the exposure conditions were different in these two periods. The natural weathering tests started in mid autumn, with winter being included in the period of zero to six months. Thus, the period of seven to 12 months (which included summer) had higher UV radiant exposure and higher temperature than the period of zero to six months, resulting in more severe degradation conditions.

Moving on to the artificial weathering tests, in the case of GT165, the AW sample had a T_{max} 22.3% lower than the reference sample. However, the 95% confidence intervals are relatively wide, which makes it difficult to conclude whether the difference is actually representative. The analysis of $\varepsilon_{T_{max}}$ helps to clarify this issue, as it clearly shows the existence of a pronounced reduction on this parameter (from 34.7% to 10.7%), proving the existence of degradation in GT165. Interestingly, no changes were found in $J_{s2\%}$ and $J_{s5\%}$.

In relation to GT375, the T_{max} of the AW sample was not different from that of the reference sample. The observed reduction of 4.0% can be considered meaningless taking into account the 95% confidence intervals. By contrast, there was a decrease in $\varepsilon_{T_{max}}$ (from 40.9% to 31.7%). As in GT165, $J_{s2\%}$ and $J_{s5\%}$ were not altered by the exposure of GT375 to artificial weathering.

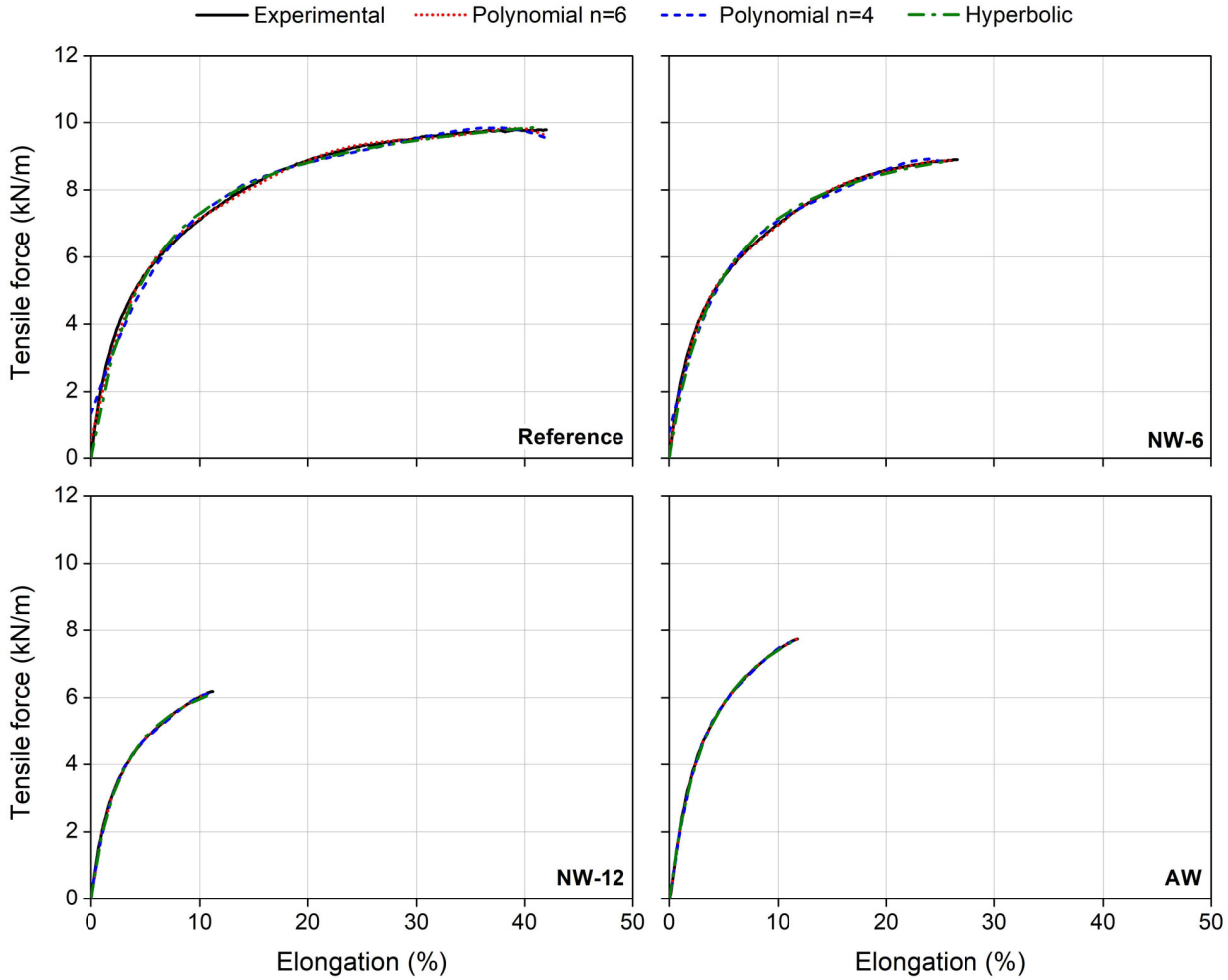

Fig. 3. Tensile force versus elongation curves of GT165 before and after the weathering tests for representative specimens: experimental curve and corresponding fitted curves with Order 4 and Order 6 polynomial equations and with hyperbolic equations.

Having characterized the behavior of GT165 and GT375 after the natural and artificial weathering tests, it becomes relevant to compare the results obtained. For both geotextiles, the exposure to natural weathering for 12 months was more damaging (higher deterioration of tensile properties) than the artificial weathering test. This outcome can be explained by the fact that the UV radiant exposure was much higher in the field than in the laboratory, i.e., 401 MJ/m^2 (estimated) compared with 50 MJ/m^2. If the temperature in the field had not been lower than in the laboratory (higher temperature promotes higher degradation in PP geotextiles), the difference would be expected to be even more pronounced. As a side note, the UV radiant exposure of 50 MJ/m^2 [used in the artificial weathering tests as recommended by EN 12224 (CEN 2000)] corresponds, in Southern Europe, to approximately one month of exposure in summer (ISO 2007).

The artificial weathering test was more damaging to GT165 than six months of natural weathering (reductions in T_{max} of 22.3% and 6.3%, respectively; decrease in $\varepsilon_{T_{max}}$ from 34.7% to, respectively, 10.7% and 25.1%). This way, the period of zero to six months (covering winter season) was less severe (even with an estimated UV radiant exposure of 101 MJ/m^2) than a UV radiant exposure of 50 MJ/m^2 in the laboratory weatherometer. The higher impact of the artificial weathering test (although with lower UV radiant exposure) can be explained by the higher temperature (50°C) at which the degradation process took place. In the case of GT375, the difference was small between artificial weathering and six months of natural weathering (reductions in $T_{max} \leq 4.0\%$ in both cases), with none causing pronounced damage. The relationships between natural and artificial weathering should be considered carefully. Indeed, they depend not only on the characteristics of the geotextiles (e.g., polymer, stabilization package, physical properties) but also on the field exposure conditions, which are variable and cannot be controlled or reproduced.

Models and Parameters

Summary of Results

The results presented herein refer to two constitutive models: polynomial equations of different order (4 and 6) and a hyperbolic model. The experimental data for each specimen were fitted with the corresponding constitutive equations, and model parameters were obtained. Figs. 3 and 4 summarize tensile force versus elongation curves obtained: experimental data for a particular specimen (selected as representative of the overall tensile response) and the respective approximations using the polynomial and hyperbolic equations. The model parameters for each sample were estimated

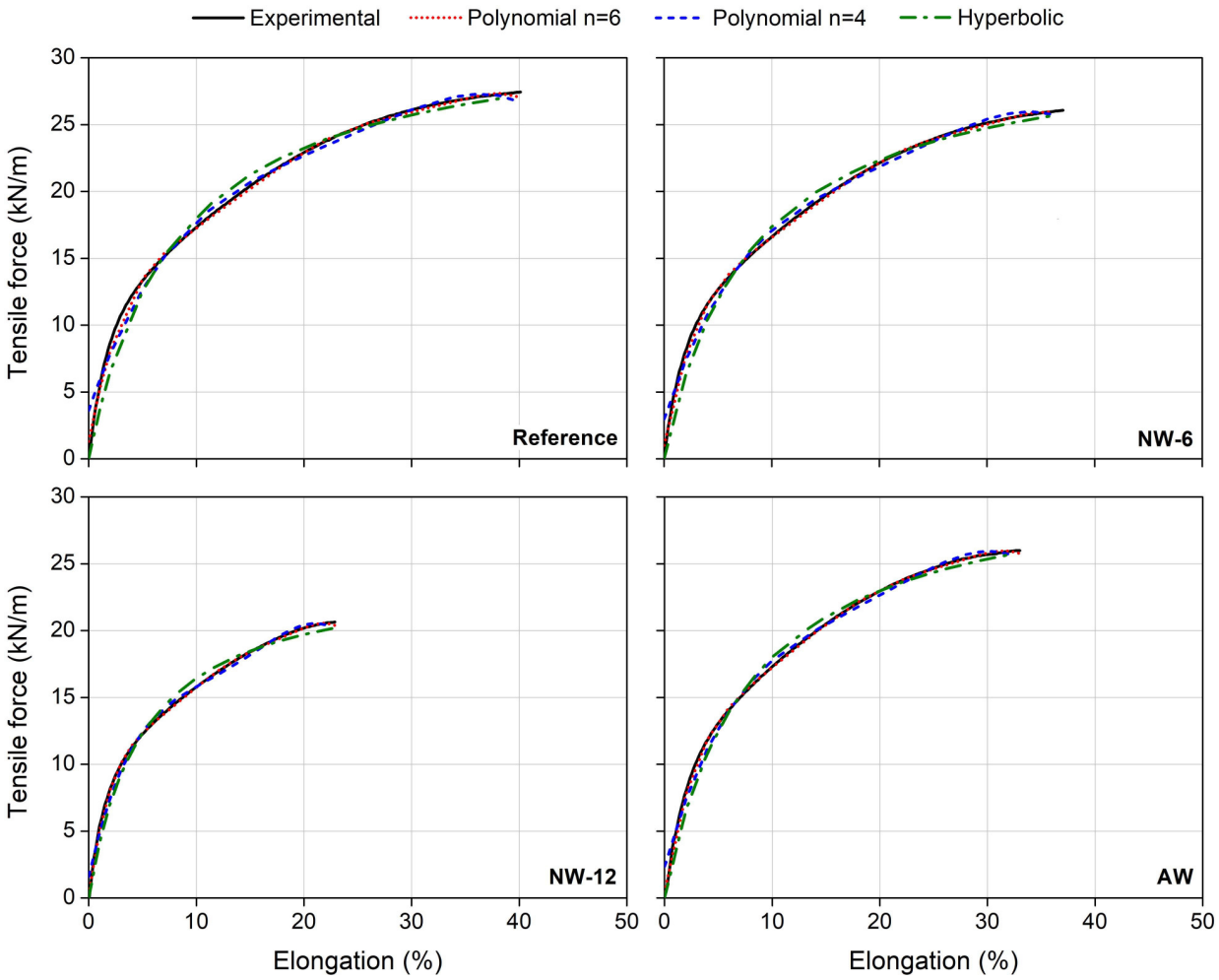

Fig. 4. Tensile force versus elongation curves of GT375 before and after the weathering tests for representative specimens: experimental curve and corresponding fitted curves with Order 4 and Order 6 polynomial equations and with hyperbolic equations.

Table 4. Model parameters for GT165 before and after the weathering tests

Model	Parameter	Reference	NW-6	NW-12	AW
Polynomial 4	a_4	-0.0000403 ± 0.0000434	-0.0001235 ± 0.0001172	-0.0011686 ± 0.0002056	-0.0015209 ± 0.0008504
	a_3	0.0029409 ± 0.0000001	0.0068400 ± 0.0000006	0.0345920 ± 0.0000149	0.0426278 ± 0.0000226
	a_2	-0.0840924 ± 0.0000878	-0.1441500 ± 0.0002580	-0.3817780 ± 0.0018098	-0.4585540 ± 0.0026109
	a_1	1.2192000 ± 0.0184567	1.5332000 ± 0.0291878	2.1318000 ± 0.0564283	2.5920000 ± 0.0834207
	a_0	1.1342000 ± 0.0159729	0.6808000 ± 0.0057550	0.1216000 ± 0.0001836	0.0091000 ± 0.0000010
	R^2	0.9926 ± 0.0122	0.9956 ± 0.0123	0.9992 ± 0.0124	0.9993 ± 0.0124
Polynomial 6	a_6	-0.0000003 ± 0.0000004	-0.0000011 ± 0.0000013	-0.0000188 ± 0.0000058	0.0006050 ± 0.0017056
	a_5	0.0000300 ± 0.0000335	0.0000852 ± 0.0000811	0.0007971 ± 0.0002112	-0.0099425 ± 0.0288257
	a_4	-0.0011910 ± 0.0010499	-0.0027056 ± 0.0018980	-0.0139315 ± 0.0030155	0.0579760 ± 0.1860045
	a_3	0.0245202 ± 0.0154299	0.0446923 ± 0.0212536	0.1302286 ± 0.0216767	-0.1031434 ± 0.5691111
	a_2	-0.2827680 ± 0.1058053	-0.4121900 ± 0.1173179	-0.7162620 ± 0.0833308	-0.3818420 ± 0.8317113
	a_1	1.9883600 ± 0.2854091	2.3136600 ± 0.3203964	2.5922000 ± 0.1681605	2.7512000 ± 0.5953474
	a_0	0.3976000 ± 0.2427613	0.1330000 ± 0.0857558	-0.0148800 ± 0.0178323	-0.0842000 ± 0.0882298
	R^2	0.9988 ± 0.0009	0.9997 ± 0.0001	0.9999 ± 0.0000	0.9998 ± 0.0001
Hyperbolic	a	0.4357420 ± 0.0309181	0.4390920 ± 0.0446681	0.4036440 ± 0.0274914	0.3536760 ± 0.0298222
	b	0.0900918 ± 0.0050405	0.0935822 ± 0.0046778	0.1242900 ± 0.0048674	0.0994588 ± 0.0122321
	R^2	0.9963 ± 0.0014	0.9964 ± 0.0011	0.9984 ± 0.0005	0.9985 ± 0.0014

Note: Average values and 95% confidence intervals.

Table 5. Model parameters for GT375 before and after the weathering tests

Model	Parameter	Reference	NW-6	NW-12	AW
Polynomial 4	a_4	-0.0000352 ± 0.0000127	-0.0000550 ± 0.0000276	-0.0003631 ± 0.0000400	-0.0001126 ± 0.0000529
	a_3	0.0033787 ± 0.0000001	0.0046869 ± 0.0000003	0.0193290 ± 0.0000046	0.0081700 ± 0.0000008
	a_2	-0.1242980 ± 0.0001918	-0.1514960 ± 0.0002850	-0.3721320 ± 0.0017195	-0.2205840 ± 0.0006042
	a_1	2.3882000 ± 0.0708183	2.5714000 ± 0.0821000	3.5536000 ± 0.1567982	3.0680000 ± 0.1168732
	a_0	3.4080000 ± 0.1442126	3.1100000 ± 0.1200950	1.6500000 ± 0.0338043	2.2660000 ± 0.0637564
	R^2	0.9925 ± 0.0122	0.9935 ± 0.0123	0.9950 ± 0.0123	0.9947 ± 0.0123
Polynomial 6	a_6	-0.0000002 ± 0.0000001	-0.0000003 ± 0.0000002	-0.0000036 ± 0.0000006	-0.0000007 ± 0.0000005
	a_5	0.0000275 ± 0.0000082	0.0000411 ± 0.0000199	0.0002790 ± 0.0000346	0.0000780 ± 0.0000402
	a_4	-0.0014591 ± 0.0003490	-0.0019797 ± 0.0007396	-0.0086958 ± 0.0007996	-0.0032617 ± 0.0013182
	a_3	0.0384350 ± 0.0070518	0.0475417 ± 0.0129024	0.1369536 ± 0.0086865	0.0687339 ± 0.0203315
	a_2	-0.5344080 ± 0.0704914	-0.6058440 ± 0.1067084	-1.1565000 ± 0.0466019	-0.7760180 ± 0.1517449
	a_1	4.3384000 ± 0.3758398	4.5322000 ± 0.4560128	5.6589400 ± 0.1454548	5.1485000 ± 0.5519151
	a_0	1.1480000 ± 0.4833248	1.0440000 ± 0.2174862	0.3240000 ± 0.0968179	0.3574000 ± 0.2497684
	R^2	0.9989 ± 0.0004	0.9991 ± 0.0004	0.9996 ± 0.0001	0.9996 ± 0.0002
Hyperbolic	a	0.2371020 ± 0.0140271	0.2380780 ± 0.0232915	0.2083740 ± 0.0071816	0.2294120 ± 0.0225573
	b	0.0313124 ± 0.0021498	0.0316100 ± 0.0032180	0.0404732 ± 0.0006843	0.0320256 ± 0.0019823
	R^2	0.9890 ± 0.0032	0.9879 ± 0.0022	0.9853 ± 0.0013	0.9895 ± 0.0038

Note: Average values and 95% confidence intervals.

Table 6. Secant and tangent stiffness of GT165 before and after the weathering tests, estimated from the constitutive models

Model	Sample	$J_{s2\%}$ (kN/m)	$J_{s5\%}$ (kN/m)	$J_{t0\%}$ (kN/m)
Polynomial 4	Reference	162.96 ± 8.20	96.87 ± 3.80	121.92 ± 24.76
	NW-6	161.17 ± 12.92	110.42 ± 7.96	153.32 ± 31.87
	NW-12	155.81 ± 7.81	96.60 ± 3.82	213.18 ± 11.70
	AW	183.78 ± 17.38	117.66 ± 11.94	259.20 ± 21.63
Polynomial 6	Reference	171.06 ± 7.58	102.41 ± 4.22	198.84 ± 28.54
	NW-6	171.42 ± 12.51	110.82 ± 6.36	231.37 ± 32.04
	NW-12	157.39 ± 7.66	96.17 ± 3.85	259.22 ± 16.82
	AW	185.69 ± 19.14	117.01 ± 11.35	275.12 ± 59.53
Hyperbolic	Reference	162.55 ± 7.77	100.57 ± 4.01	230.10 ± 16.35
	NW-6	160.22 ± 13.19	110.51 ± 7.42	229.02 ± 24.18
	NW-12	153.51 ± 7.40	97.64 ± 4.03	248.31 ± 16.18
	AW	181.72 ± 16.20	118.11 ± 11.76	283.79 ± 23.85

Note: Average values and 95% confidence intervals.

by averaging the corresponding model parameters obtained for each specimen tested. The average values of the model parameters and the coefficient of determination (R^2) of the curve fitting exercise are included in Tables 4 and 5 for GT165 and GT375, respectively. From the constitutive models and using Eqs. (5) and (6), the secant and tangent stiffness were estimated (Tables 6 and 7).

Polynomial Model

Using representative curves and their corresponding estimates, Figs. 3 and 4 illustrate how well polynomial models of Orders 4 and 6 fit the experimental data and were able to reproduce the changes in response associated to the weathering induced in GT165 and GT375. The quality of the approximation is confirmed by the

Table 7. Secant and tangent stiffness of GT375 before and after the weathering tests, estimated from the constitutive models

Model	Sample	$J_{s2\%}$ (kN/m)	$J_{s5\%}$ (kN/m)	$J_{t0\%}$ (kN/m)
Polynomial 4	Reference	385.68 ± 27.25	252.84 ± 15.55	238.82 ± 23.50
	NW-6	384.17 ± 29.17	225.15 ± 18.29	257.14 ± 30.72
	NW-12	370.87 ± 8.72	246.08 ± 5.02	355.36 ± 8.62
	AW	379.16 ± 19.79	230.05 ± 14.36	306.80 ± 42.38
Polynomial 6	Reference	398.61 ± 27.27	269.10 ± 16.45	433.84 ± 37.58
	NW-6	401.75 ± 30.03	241.12 ± 19.05	453.22 ± 45.60
	NW-12	399.05 ± 10.66	244.13 ± 5.51	565.89 ± 14.55
	AW	402.52 ± 22.07	243.52 ± 12.71	514.85 ± 55.19
Hyperbolic	Reference	334.24 ± 20.12	254.49 ± 15.25	422.56 ± 26.11
	NW-6	333.34 ± 30.52	220.37 ± 19.44	422.16 ± 42.00
	NW-12	345.78 ± 9.60	243.53 ± 5.64	480.20 ± 16.66
	AW	341.90 ± 28.03	224.30 ± 15.37	438.29 ± 46.86

Note: Average values and 95% confidence intervals.

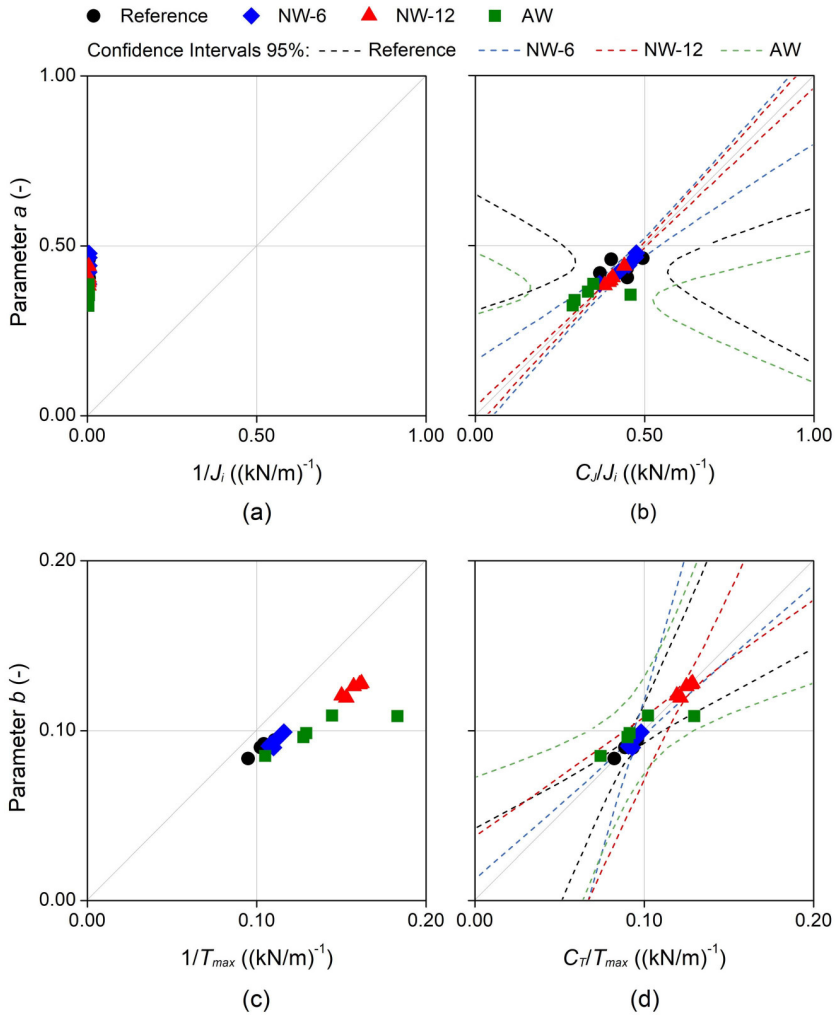

Fig. 5. Physical meaning of hyperbolic model parameters, GT165: (a) parameter a versus $1/J_i$; (b) parameter a versus $1/J_i$ with correction factor C_J; (c) parameter b versus $1/T_{max}$; and (d) parameter b versus $1/T_{max}$ with correction factor C_T.

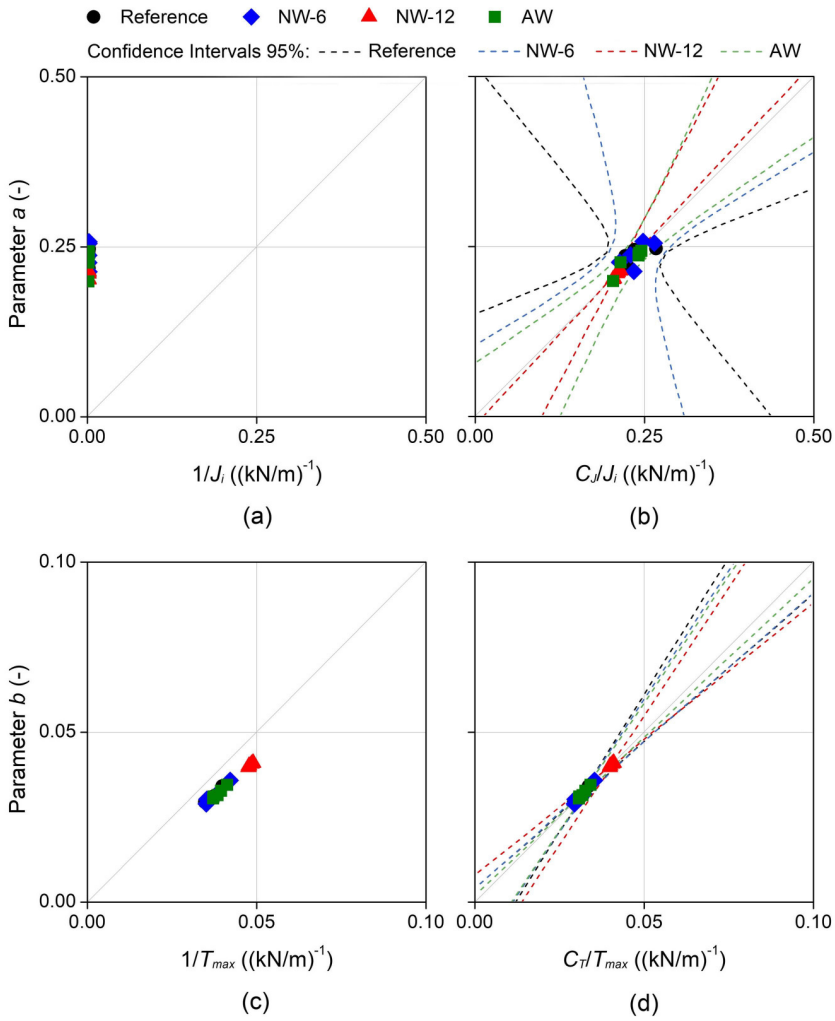

Fig. 6. Physical meaning of hyperbolic model parameters, GT375: (a) parameter a versus $1/J_i$; (b) parameter a versus $1/J_i$ with correction factor C_J; (c) parameter b versus $1/T_{\max}$; and (d) parameter b versus $1/T_{\max}$ with correction factor C_T.

average values of R^2, which ranged between 0.9925 and 0.9999, and their reduced dispersion (Tables 4 and 5). The coefficients a_i, i.e., the model parameters, have no physical meaning. In general, high-order polynomials improve the efficiency of estimates. In this particular case, there was no significant improvement when using Order 6 polynomials instead of Order 4 polynomials. This is confirmed by the values of R^2 of the approximations and by the low values of the Orders 5 and 6 coefficients, a_5 and a_6, of the polynomial model of Order 6. Thus, the lower-order polynomials considered ($n = 4$) were able to provide sufficient approximation of the experimental data of both GT165 and GT375.

The secant stiffness for 2% and 5% elongation, $J_{s2\%}$ and $J_{s5\%}$, obtained from the polynomial models (Tables 6 and 7) are good, though mostly lower, estimates of the experimental data. For example, the estimates of $J_{s2\%}$ obtained with the Order 4 polynomials are 1.2% to 10.4% lower relative to the experimental data, while the estimates of $J_{s5\%}$ are 0.9% higher to 15.6% lower than the test results. Similar estimates obtained from the Order 6 polynomials have a smaller variation relative to the experimental results: 0.2% to 6.5% lower than the experimental data for $J_{s2\%}$ and 0.4% higher to 9.6% lower for $J_{s5\%}$.

Overall, the polynomial equations provided a good approximation of the experimental results. Thus, they were able to reproduce the trends discussed for the tensile results.

Hyperbolic Model

The experimental data were fitted well by the hyperbolic models (Figs. 3 and 4; Tables 4 and 5), with R^2 ranging between 0.9853 and 0.9985. One of the advantages of using hyperbolic models is their relation to the tensile properties of geosynthetics [Eqs. (3) and (4)]. From Figs. 5 and 6, it is clear that those relations are not fully applicable, in particular for parameter a and J_i. Because $J_{t0\%}$ cannot be measured directly from the experimental data, herein, J_i values were estimated using the Order 6 polynomial models as the tangent stiffness for 0% elongation ($J_{t0\%}$). Often, in the application of hyperbolic models, a failure ratio (constant to approximate the data to the asymptote of the hyperbolic equation) is included. A similar approach was employed herein, and equivalent ratios were applied, designated as correction factors. These factors, C_J and C_T, were applied to parameters a and b, respectively [Eqs. (7) and (8)] and are summarized in Table 8. Figs. 5 and 6, for GT165 and GT375, respectively, illustrate the need for the correction factors

for the reference and weathered samples. Only the correction factor C_T is truly a failure ratio

$$a = \frac{C_J}{J_i} \tag{7}$$

$$b = \frac{C_T}{T_{\max}} \tag{8}$$

These correction factors (Table 8) are not material constants, as they changed after the weathering induced and depended on the geotextile, the type of weathering and, for the natural weathering, on the period of exposure. For the reference sample of GT165: $C_J = 85.01$ and $C_T = 0.867$; for the reference sample of GT375: $C_J = 102.14$ and $C_T = 0.842$. Regardless of the weathering conditions, the correction factor C_J increased after weathering (variation between 5% to 23%), while the correction factor C_T decreased (variation between –0.5% to –18%). For the weathered samples, the correction factor C_T (i.e., a failure ratio) was reduced relative to the reference samples and ranged between 0.707 and 0.845 for GT165 and between 0.827 and 0.838 for GT375.

Table 8. Correction factors C_J and C_T

Geotextile	Sample	C_J	R^2 for C_J	C_T	R^2 for C_T
GT165	Reference	85.01	0.9904	0.867	0.9995
	NW-6	100.49	0.9994	0.845	0.9998
	NW-12	104.40	1.0000	0.794	0.9999
	AW	92.05	0.9735	0.707	0.9862
GT375	Reference	102.14	0.9970	0.842	0.9999
	NW-6	107.15	0.9969	0.838	0.9998
	NW-12	117.89	0.9999	0.838	1.0000
	AW	117.37	0.9993	0.827	0.9999

Fig. 5 (GT165) and 6 (GT375) include lines representing the 95% confidence interval for the correction factors for a and b. For C_J, the 95% confidence interval is wide, as a consequence of the scatter of the values of J_i obtained for the different specimens tested per condition. Conversely, for C_T, the 95% confidence interval is narrow, particularly for GT375.

As for the polynomial models, the secant stiffness for 2% and 5% elongation, $J_{s2\%}$ and $J_{s5\%}$, were estimated from the hyperbolic models (Tables 6 and 7). The corresponding estimated values were close to the experimental data, although always lower.

Estimating Model Parameters for Weathered Samples

One of this study's main objectives was to implement simple relations to estimate model parameters for weathered samples from tensile properties of reference and weathered samples. Although Order 4 and 6 polynomial models provided good fit of the experimental data, the results showed that the polynomial model parameters had no physical meaning, which constitutes the main limitation of these models. Thus, to relate the weathering conditions and the observed tensile response of GT165 and G375, links among the correction factors, hyperbolic-model parameters a and b, and the reduction factors for weathering were investigated.

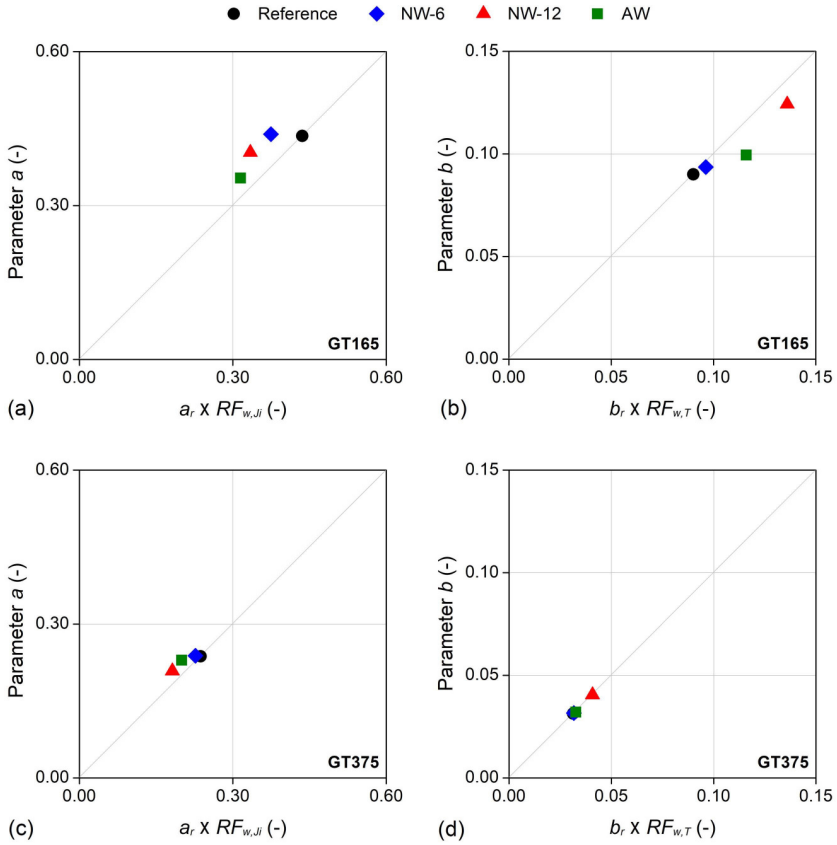

Fig. 7. Analysis for estimating model parameters after weathering: (a) GT165 parameter a versus $a_r \times RF_{w,Ji}$; (b) GT165 parameter b versus $b_r \times RF_{w,T}$; (c) GT375 parameter a versus $a_r \times RF_{w,Ji}$; and (d) GT375 parameter b versus $b_r \times RF_{w,T}$.

The reduction factor for the initial stiffness to allow for weathering ($RF_{w,Ji}$) is represented by Eq. (9) that relates the initial stiffness of the reference sample ($J_{i,r}$) to that obtained after weathering ($J_{i,w}$). The reduction factor for the tensile strength to allow for weathering ($RF_{w,T}$) is represented by Eq. (10), which relates the tensile strength of the reference sample ($T_{\max,r}$) to that obtained after weathering ($T_{\max,w}$)

$$RF_{w,Ji} = \frac{J_{i,r}}{J_{i,w}} \tag{9}$$

$$RF_{w,T} = \frac{T_{\max,r}}{T_{\max,w}} \tag{10}$$

The most promising relations found for estimating the hyperbolic model parameters after weathering are summarized in Fig. 7.

As shown in Figs. 7(a) and 7(c), combining the model parameter a for the reference sample (a_r) and the reduction factor for the initial stiffness ($RF_{w,Ji}$) gives a reasonable, though low, estimate ($a_{w,e}$) of parameter a of the weathered samples (a_w), represented in Eq. (11). Such estimate is better for GT375 than for GT165

$$a_w \sim a_{w,e} = a_r \times RF_{Ji,w} \tag{11}$$

Similarly, Figs. 7(b) and 7(d) shows that combining the model parameter b for the reference sample (b_r) and the reduction factor for the tensile strength ($RF_{w,T}$) gives a reasonable estimate ($b_{w,e}$) of parameter b of the weathered samples (b_w), represented in Eq. (12). For GT165, these estimates were higher than the model parameters derived, while for GT375 there were no relevant differences

$$b_w \sim b_{w,e} = b_r \times RF_{T,w} \tag{12}$$

To confirm the quality of these estimates, tensile force versus elongation curves using hyperbolic equations were estimated for the different types of samples and were represented and compared with the experimental data (Figs. 8 and 9, for GT165 and GT375, respectively). The quality of the estimates depends on the geotextile and on the estimated model parameters $a_{w,e}$ and $b_{w,e}$ obtained from Eqs. (11) and (12). Considering the scatter of experimental data, the estimated hyperbolic curves fit adequately the experimental data, particularly for low elongation (<3%).

With the procedure described, it is possible to have an estimate of model parameters for weathered samples from tensile properties of reference and weathered samples. These estimates rely on the knowledge of the reduction factors for weathering. If these factors are not known, databases may be a useful source of reduction factor

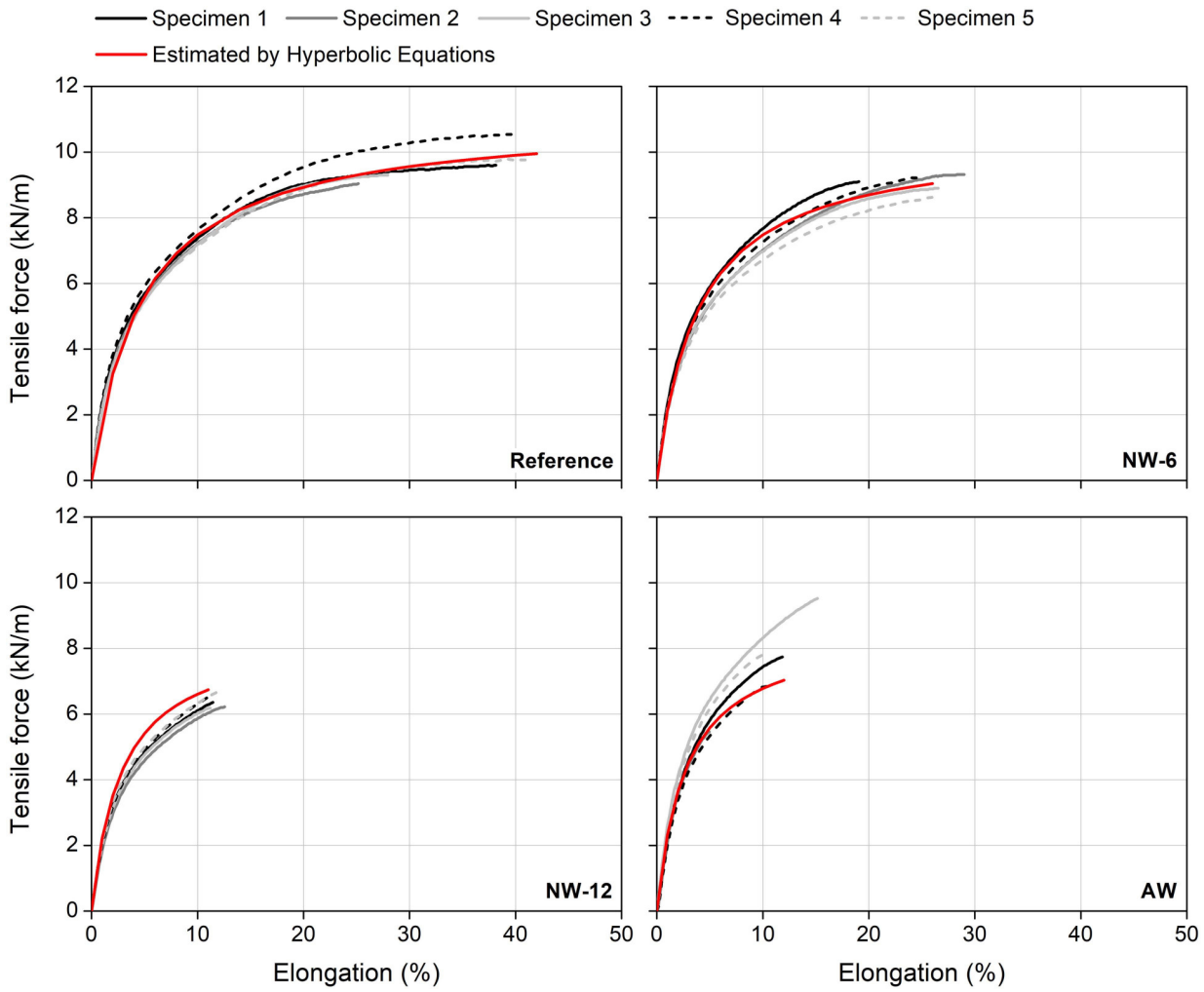

Fig. 8. Tensile force versus elongation curves of GT165 before and after the weathering tests: experimental (five specimens) and estimated by hyperbolic equations.

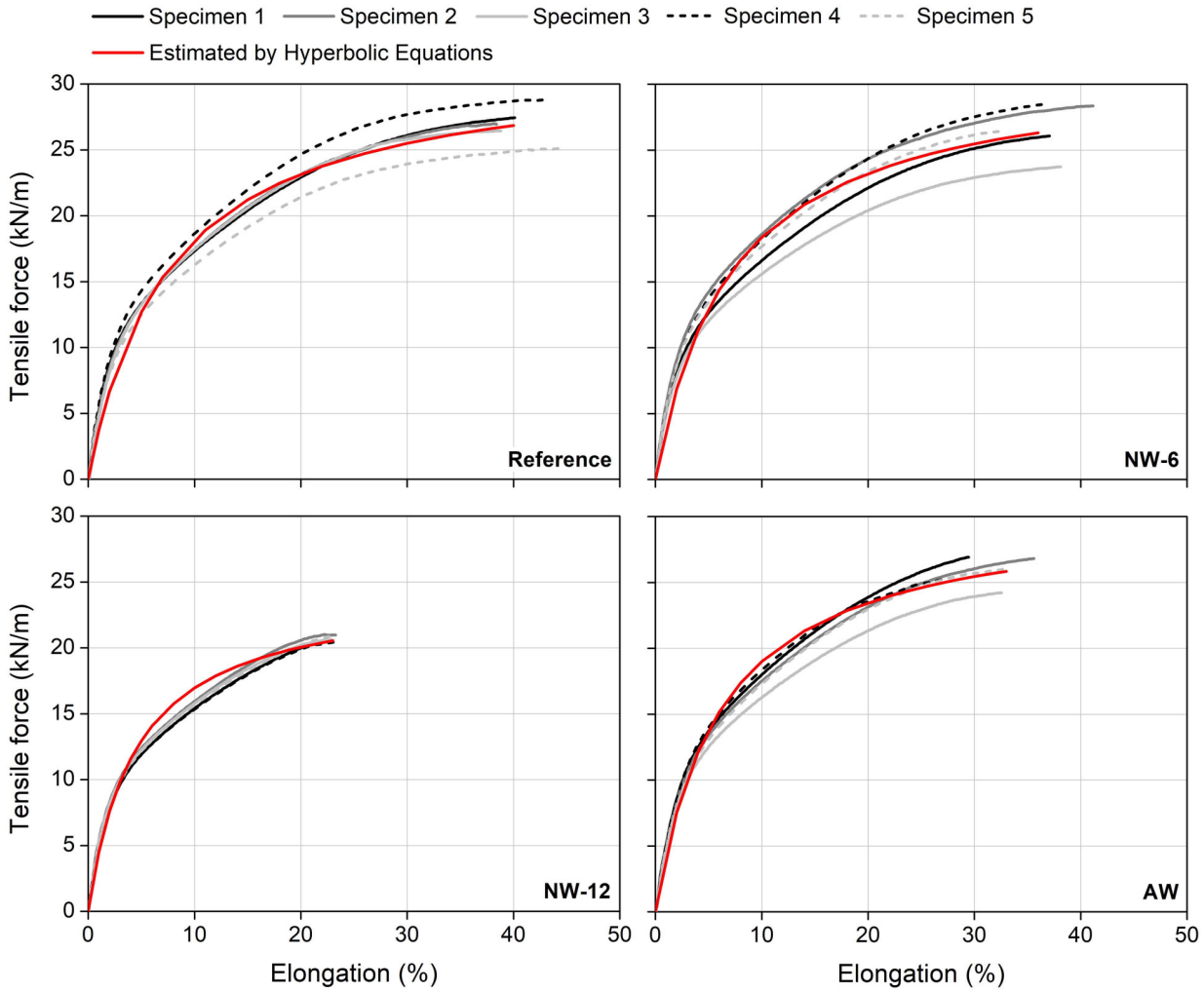

Fig. 9. Tensile force versus elongation curves of GT375 before and after the weathering tests: experimental (five specimens) and estimated by hyperbolic equations.

values for an initial estimate. Examples of values for reduction factors allowing for durability can be found in Greenwood et al. (2016).

The proposed process can be summarized as

1. Characterize the full tensile response of a chosen geotextile (reference sample).
2. Use curve fitting to approximate that response by a hyperbolic equation and derive the corresponding model parameters (a_r, b_r); these can be related to J_i and $T_{\max}$.
3. Obtain the reduction factors for J_i and $T_{\max}$ after weathering (from laboratory or field tests, or from the literature, depending on the actual objective of the analysis): $RF_{Ji,w}$, $RF_{T,w}$.
4. Using the proposed equations [Eqs. (11) and (12)], estimate the model parameters for the weathered sample (a_{we}, b_{we})
5. Implement the estimated hyperbolic equation for the weathered sample on the numerical software.

The approach described herein allowed estimating adequately the response of weathered samples using tensile tests results of both reference and weathered samples, combined with model parameters for the reference sample. This approach contributes to defining simple models, which can be implemented in software, and, ultimately, will lead to using more realistic responses of geotextiles in their design.

Conclusions

The tensile force versus elongation response of two thermally bonded polypropylene geotextiles, before and after weathering, was assessed experimentally and then analyzed using two different constitutive models, polynomial (Orders 4 and 6) and hyperbolic. Two natural weathering conditions with different exposure times were considered as well as artificial weathering.

The initial objectives of this work were achieved: the influence of weathering on the tensile force versus elongation response of two geotextiles was analyzed and discussed; simple constitutive models for representing the tensile force versus elongation response were adopted and the corresponding model parameters were derived; simple relations were implemented to estimate model parameters for weathered samples from tensile properties of reference and weathered samples.

The six months of natural weathering had a relatively small impact on the tensile behavior of the geotextiles. However, with the increase of the exposure time to 12 months, some meaningful changes were observed in their properties. In the natural and artificial weathering tests, the geotextile with the highest mass per unit area and thickness showed slightly better resistance to weathering. For both geotextiles, 12 months of natural weathering were more

damaging than the ≈15 day artificial weathering test. The same did not occur when compared with the exposure time of six months.

The results confirmed that, although polynomial models fit the experimental data very well, the model parameters had no link to the tensile properties of the geotextiles, which limits their application. Though, in general, high-order polynomials improve the efficiency of estimates, for the geotextiles studied there was no significant improvement when using Order 6 polynomials instead of Order 4 polynomials.

Hyperbolic models were the most promising, as they were able to fit the experimental data adequately and the model parameters linked to tensile properties of the geotextiles, particularly if affected by correction factors. These corrections factors were not material constants.

The hyperbolic model parameters of the samples submitted to weathering were estimated using the model parameters for the reference samples and the reduction factor to allow for weathering for the initial stiffness and the tensile strength. These estimates were found adequate for representing the tensile response of the weathered samples, particularly for low ranges of elongation.

Herein, a simple procedure that can be used to estimate model parameters for representing the tensile response of weathered geotextiles was shown. Although this approach needs to be confirmed for more geosynthetics and weathering conditions, it is promising in generating realistic tensile force versus elongation curves. These estimated models may be implemented in software using finite element or finite differences methods.

Currently, the tensile response of geotextiles is mostly represented by a linear elastic constitutive model, with a constant stiffness, and corresponding to the behavior of reference samples. Ultimately, the approach proposed herein will enable representing that tensile response more realistically. This is a result of the ability of hyperbolic models to represent the change of stiffness as a function of the level of elongation. In addition, that representation can consider the changes of response associated to weathering, particularly for elongations typical of service.

Data Availability Statement

Some or all data, models, or code that support the findings of this study are available from the corresponding author upon reasonable request.

Acknowledgments

This work was financially supported by (1) Base Funding, UIDB/04708/2020 of the CONSTRUCT, Instituto de I&D em Estruturas e Construções, funded by national funds through the FCT/MCTES (PIDDAC); and (2) Foundation for Science and Technology (FCT), Aveiro Research Centre for Risks and Sustainability in Construction (RISCO), Universidade de Aveiro, Portugal [FCT/UIDB/ECI/04450/2020].

Notation

The following symbols are used in this paper:

a = hyperbolic model parameter a;
a_i = polynomial model parameter of order i;
a_r = hyperbolic model parameter a of the reference sample;
a_w = hyperbolic model parameter a of the weathered sample;
$a_{w,e}$ = hyperbolic model parameter a of the weathered sample (estimated);
a_5 = polynomial model parameter of Order 5;
a_6 = polynomial model parameter of Order 6;
b = hyperbolic model parameter b;
b_r = hyperbolic model parameter b for the reference sample;
b_w = hyperbolic model parameter b for the weathered sample;
$b_{w,e}$ = hyperbolic model parameter b for the weathered sample (estimated);
C_J = correction factor for the stiffness;
C_T = correction factor for the tensile strength;
E = accumulated solar radiant energy;
E_{UV} = accumulated UV radiant energy;
J = instantaneous tangent stiffness;
J_i = initial tangent stiffness;
$J_{i,r}$ = initial tangent stiffness of the reference sample;
$J_{i,w}$ = initial tangent stiffness of the weathered sample;
$J_{s2\%}$ = secant stiffness at 2% elongation;
$J_{s5\%}$ = secant stiffness at 5% elongation;
$J_{t0\%}$ = tangent stiffness at 0% elongation;
n = order of the polynomial equation;
P = accumulated precipitation;
R^2 = coefficient of determination;
$RF_{w,Ji}$ = reduction factor for the initial stiffness to allow for weathering;
$RF_{w,T}$ = reduction factor for the tensile strength to allow for weathering;
T = tensile force;
$T_{\mathrm{air,avg}}$ = daily average air temperature: average;
$T_{\mathrm{air,max}}$ = daily average air temperature: maximum;
$T_{\mathrm{air,min}}$ = daily average air temperature: minimum;
T_{max} = tensile strength;
$T_{\mathrm{max},r}$ = tensile strength of the reference sample;
$T_{\mathrm{max},w}$ = tensile strength of the weathered sample;
t = thickness;
ε = elongation;
$\varepsilon_{T\mathrm{max}}$ = elongation at tensile strength; and
μ_{A} = mass per unit area.

References

Aparicio-Ardila, M. A., G. O. M. Pedroso, M. Kobelnik, C. A. Valentin, M. P. Luz, and J. F. Silva. 2021. "Evaluating the degradation of a nonwoven polypropylene geotextile exposed to natural weathering for 3 years." *Int. J. Geosynth. Ground Eng.* 7 (21): 69. https://doi.org/10.1007/s40891-021-00314-6.

ASTM. 2021. *Standard test method for deterioration of geotextiles by exposure to light, moisture, and heat in a xenon-arc-type apparatus*. ASTM D4355. West Conshohocken, PA: ASTM.

Bathurst, R. J., and V. N. Kaliakin. 2005. "Review of numerical models for geosynthetics in reinforcement applications." In *Proc., 11th Int. Conf. Int. Association Computational Methods Advance Geomechanics*, 407–416. Torino, Italy: International Association for Computer Methods and Advances in Geomechanics.

BSI (British Standards Institution). 2010. *Code of practice for strengthened/reinforced soils and other fills*. BS 8006-1. London: BSI.

Buljak, V., and G. Ranzi. 2021. *Constitutive modeling of engineering materials: Theory, computer implementation, and parameter identification*. London: Academic Press.

Carneiro, J. R., P. J. Almeida, and M. L. Lopes. 2011. "Accelerated weathering of polypropylene geotextiles." *Sci. Eng. Compos. Mater.* 18 (4): 241–245. https://doi.org/10.1515/SECM.2011.047.

Carneiro, J. R., P. J. Almeida, and M. L. Lopes. 2019. "Evaluation of the resistance of a polypropylene geotextile against ultraviolet radiation." *Microsc. Microanal.* 25 (1): 196–202. https://doi.org/10.1017/S1431927618000430.

Carneiro, J. R., and M. L. Lopes. 2017. "Natural weathering of polypropylene geotextiles treated with different chemical stabilisers." *Geosynth. Int.* 24 (6): 544–553. https://doi.org/10.1680/jgein.17.00020.

CEN (European Committee for Standardization). 1992. *Textiles—Test methods for nonwovens—Part 3: Determination of tensile strength and elongation*. EN 29073-3. Brussels, Belgium: CEN.

CEN (European Committee for Standardization). 2000. *Geotextiles and geotextile-related products—Determination of the resistance to weathering*. EN 12224. Brussels, Belgium: CEN.

CEN (European Committee for Standardization). 2005a. *Geosynthetics—Sampling and preparation of test-specimens*. EN ISO 9862. Brussels, Belgium: CEN.

CEN (European Committee for Standardization). 2005b. *Geosynthetics—Test method for the determination of mass per unit area of geotextiles and geotextile-related products*. EN ISO 9864. Brussels, Belgium: CEN.

CEN (European Committee for Standardization). 2013. *Geosynthetic barriers—Characteristics required for use in the construction of canals*. EN 13362. Brussels, Belgium: CEN.

CEN (European Committee for Standardization). 2016. *Geosynthetics—Determination of thickness at specified pressures—Part 1: Single layers*. EN ISO 9863-1. Brussels, Belgium: CEN.

Feldman, D. 2002. "Polymer weathering: Photo-oxidation." *J. Polym. Environ.* 10 (4): 163–173. https://doi.org/10.1023/A:1021148205366.

Filho, J. L. E. D., P. C. A. Maia, and G. C. Xavier. 2019. "Spectrophotometry as a tool for characterizing durability of woven geotextiles." *Geotext. Geomembr.* 47 (4): 577–585. https://doi.org/10.1016/j.geotexmem.2019.02.002.

Franco, Y. B., C. A. Valentin, M. Kobelnik, J. L. Silva, C. A. Ribeiro, and M. P. Luz. 2022. "Accelerated aging ultraviolet of a PET nonwoven geotextile and thermoanalytical evaluation." *Materials (Basel)* 15 (12): 4157. https://doi.org/10.3390/ma15124157.

Giroud, J. P., J. Han, E. Tutumluer, and M. J. D. Dobie. 2022. "The use of geosynthetics in roads." *Geosynth. Int.* 30 (1): 47–80. https://doi.org/10.1680/jgein.21.00046.

Greenwood, J. H., H. F. Schroeder, and W. Voskamp. 2016. *Durability of geosynthetics*. Boca Raton, FL: CRC Press.

Han, J. 2015. *Principles and practices of ground improvement*. Hoboken, NJ: Wiley.

Hsieh, C., J.-B. Wang, and Y.-F. Chiu. 2006. "Weathering properties of geotextiles in ocean environments." *Geosynth. Int.* 13 (5): 210–217. https://doi.org/10.1680/gein.2006.13.5.210.

ISO (International Organization for Standardization). 2007. *Guidelines for the determination of the long-term strength of geosynthetics for soil reinforcement*. ISO/TR 20432. Geneva: ISO.

Koerner, R. M. 2012. *Designing with geosynthetics*. Milton Keynes, UK: Xlibris Corporation.

Koerner, R. M., Y. G. Hsuan, and G. R. Koerner. 2017. "Lifetime predictions of exposed geotextiles and geomembranes." *Geosynth. Int.* 24 (2): 198–212. https://doi.org/10.1680/jgein.16.00026.

Liu, H., and H. I. Ling. 2006. "Modeling cyclic behavior of geosynthetics using mathematical functions combined with Masing rule and bounding surface plasticity." *Geosynth. Int.* 13 (6): 234–245. https://doi.org/10.1680/gein.2006.13.6.234.

Lombardi, G., A. M. Paula, and M. Pinho-Lopes. 2022. "Constitutive modelling and statistical analysis of the short-term tensile response of geosynthetics after damage." *Constr. Build Mater.* 317 (Jun): 125972. https://doi.org/10.1016/j.conbuildmat.2021.125972.

Maier, C., and T. Calafut. 1998. *Polypropylene. The definitive user's guide and databook*. New York: Plastics Design Library.

Paula, A. M., and M. Pinho-Lopes. 2021. "Constitutive modelling of short-term tensile response of geotextile subjected to mechanical and abrasion damages." *Int. J. Geosynth. Ground Eng.* 7 (Jun): 67. https://doi.org/10.1007/s40891-021-00313-7.

Perkins, S. W. 2000. "Constitutive modeling of geosynthetics." *Geotext. Geomembr.* 18 (5): 273–292. https://doi.org/10.1016/S0266-1144(99)00021-7.

Pinkus, A. 2000. "Weierstrass and approximation theory." *J. Approximation Theory* 107 (1): 1–66. https://doi.org/10.1006/jath.2000.3508.

Rowe, R. J. 2020. "Protecting the environment with geosynthetics: 53rd Karl Terzaghi Lecture." *J. Geotech. Geoenviron. Eng.* 146 (9): 04020081. https://doi.org/10.1061/(ASCE)GT.1943-5606.0002239.

Shukla, S. K. 2016. *An introduction to geosynthetic engineering*. Leiden, Netherlands: CRC Press.

Sprague, C. J., and J. E. Sprague. 2016. "Geosynthetics in erosion and sediment control." In *Geotextiles: From design to applications*. Sawston, UK: Woodhead Publishing.

Touze-Foltz, N., H. Bannour, C. Barral, and G. Stoltz. 2016. "A review of the performance of geosynthetics for environmental protection." *Geotext. Geomembr.* 44 (5): 656–672. https://doi.org/10.1016/j.geotexmem.2016.05.008.

Valente, I. M., J. R. Carneiro, P. J. Almeida, and M. L. Lopes. 2011. "Determination of Chimassorb 944 in polypropylene geotextiles by HPLC-UV." *Anal. Lett.* 44 (4): 617–625. https://doi.org/10.1080/00032711003783093.